Joint Entropy-assisted Graphene Oxide-based Multiplexing Biosensing Platform for Simultaneous Detection of Multiple Proteases

Youwen Zhang[1], Xiaohan Chen[1], Shaoqing Yuan[2], Liang Wang[3,4,*], and Xiyun Guan[1,*]

[1]Department of Chemistry, Illinois Institute of Technology, 3101 S Dearborn St, Chicago, IL 60616, USA
[2]Amazon, 2121 7th Ave, Seattle, WA, 98121, USA
[3]Chongqing Institute of Green and Intelligent Technology, Chinese Academy of Sciences, Chongqing 400714, China
[4]The University of Chinese Academy of Science, Beijing, 100049, China

Corresponding authors' E-mail: xguan5@iit.edu; wangliang83@cigit.ac.cn

Supporting Information

ABSTRACT: Due to the limited clinical utility of individual biomarkers, there is growing recognition of the need for combining multiple biomarkers as a panel to improve the accuracy and efficacy of disease diagnosis and prognosis. The conventional method to detect multiple analyte species is to construct a sensor array, which is consisted of an array of individual selective probes for different species. In this work, by using cancer biomarker matrix metalloproteinases (MMPs) and a disintegrin and metalloproteinases (ADAMs) as model analytes and functionalized nano-graphene oxide (nGO) as a sensing element, we developed a multiplexing fluorescence sensor in a non-array format for simultaneous measurement of the activities of multiple proteases. The constructed nGO-based biosensor was rapid, sensitive and selective, and was also utilized for the successful profiling of ADAMs/MMPs in simulated serum samples. Furthermore, we showed that joint entropy and programming could be utilized to guide experiment design, especially in terms of the selection of a subset of proteases from the entire MMPs/ADAMs family as an appropriate biomarker panel. Our developed nGO-based multiplex sensing platform should find useful application in early cancer detection and diagnosis.

Keywords: MMPs, ADAMs, Cancer Biomarker, Graphene Oxide, Non-array format, Multiplexing Biosensor, Human Serum

INTRODUCTION

Cancer is a multistage process that often involves defects and/or alterations in many major cellular pathways. Accordingly, individual biomarkers have very limited indicative value since one biomarker only represents one aspect of carcinogenesis[1]. In order to improve the accuracy and efficacy, and to minimize false positives, there is growing recognition of the need for a panel of cancer markers rather than one specific biomarker for cancer diagnosis and prognosis. The conventional method to simultaneously detect and quantitate multiple analyte species is to construct a sensor array, which is consisted of an array of individual highly selective (or specific) probes for different species[2,3]. Herein, we report an innovative multiplexing sensor in a non-array format for concurrent detection of multiple analytes. Compared with single-analyte measurement systems, simultaneous detection of multiple species in a single assay has many advantages, including reduced assay costs, improved turnaround time, reduced sample/reagent volume, high-throughput screening, and decrease in errors between inter-sampling. In this work, we use matrix metalloproteinases (MMPs) and ADAMs (short for a disintegrin and metalloproteinase) as model analyte species and the functionalized graphene oxide (GO) as a sensing element for proof-of-concept demonstration of this new multiplex sensing platform.

MMPs are a family of more than 20 zinc-dependent endopeptidases that share a similar structure and are collectively capable of degrading all components of the extracellular matrix and basement membrane[4-6]. They play important roles in cell biological processes and are involved in many fundamental physiological events such as tissue remodeling, angiogenesis, wound healing, bone development, and mammary involution. Dysregulated activities of MMPs may lead to a number of pathological conditions including tumor growth, invasion and metastasis[7-9]. ADAMs are a family of more than 30 integral membrane and secreted glycoproteins which are related to snake venom metalloproteases and MMPs[10]. ADAMs play important roles in cell surface remodeling, ectodomain shedding, regulation of growth factor availability, and in mediating cell-cell and cell-matrix interactions in both normal development and pathological states such as Alzheimer's diseases, cancer, arthritis, and cardiac hypertrophy[11-13]. Similar to MMPs, most ADAMs contain the conserved Zn-binding catalytic domain and are proteolytically active. Elevated activity levels of MMPs and/or ADAMs have been observed in almost every type of human cancers, and found to be correlated with advanced tumor stage, increased invasion and metastasis, and shortened survival[14-20]. The type of cancer and its corresponding MMPs/ADAMs detected in tumor or serum samples are summarized in Table S1 (Supporting Information). Given the significantly elevated ac-

tivity levels observed in cancer patients over other diseases and healthy controls, MMPs/ADAMs have become novel biomarkers and potential therapeutic targets for the early detection and treatment of human cancers. For example, a number of MMP inhibitors have been developed and are currently being tested in all three phases of clinical trials against a variety of human cancers[21-23]. Further, evidence is emerging that MMPs/ADAMs can also be utilized as indicators of tumor recurrence and response to cancer therapy[5,24].

Thus far, several strategies have been developed to detect MMPs/ADAMs. These include enzyme-linked immunosorbent assays (ELISA)[25], gelatinase zymography[26], surface plasmon resonance (SPR)[27], tandem mass spectrometry[28], nuclear magnetic resonance (NMR)[29], electrochemical[30] and nanopore biosensors[31]. Although these methods can provide sensitive and accurate protease detection, most of them are time-consuming and/or require the use of expensive and complicated instruments, and hence are not suitable for point-of-care applications. Fluorescence resonance energy transfer (FRET), which relies on the distance-dependent transfer of energy from a donor molecule to an acceptor molecule, has been widely used to study molecular interaction and biomolecule conformational change as well as to develop biosensors due to its high sensitivity, simplicity and reproducibility[32-34]. In this work, by taking advantage of GO, we developed a fluorescence-based multiplex sensing platform for simultaneous detection of the activities of multiple MMPs/ADAMs. As a chemically exfoliated graphene derivative, GO has an improved water solubility over graphene due to the incorporation of oxygenated groups on its basal plane and exposed edges. GO also supplies a mass of chemical binding sites for additional element conjugation[35]. Furthermore, it has been demonstrated to be an efficient quencher for various fluorophores with excellent quenching distance, thus providing opportunities to detect large biomolecules[36]. Moreover, its nontoxic and biocompatible properties offer the potential for clinical diagnosis and therapy[32]. In addition, we showed that joint entropy and programming could be utilized to guide experiment design, especially in terms of the selection of a subset of proteases from the entire MMPs/ADAMs family as an appropriate biomarker panel.

EXPERIMENTAL SECTION

Materials and reagents. ADAM-8, ADAM-9, ADAM10 and ADAM-17 were purchased from R&D Systems (Minneapolis, MN). FAM-labeled ADAM-17 protease substrate peptide (Pep-FAM) with a sequence of NH_2-CALNNLAQAV-RSSSARK(FAM) (95.22% pure) was synthesized from WatsonBio Sciences (Houston, TX), while the MCA-labeled ADAM-10 protease substrate peptide (Pep-MCA) with a sequence of NH_2-CALNNKPLGL-ARK(MCA) (96.75% pure) and TAMRA-labeled MMP-9 protease substrate peptide (Pep-TAMRA) with a sequence of NH_2-CALNNGGPRS-LSGK(TAMRA) (98.88% pure) were purchased from Biomatik corporation (Wilmington, DE). Nano-graphene oxide (nGO, diameter: 90 nm - 200 nm; thickness: ~ 1 nm) was bought from Graphene Laboratories Inc. (Ronkonkoma, NY). All the other chemicals, including MMP-9 were obtained from Sigma-Aldrich (St. Louis, MO). All the proteases and their substrate peptides were dissolved in HPLC-grade water (ChromAR, Mallinckrodt Baker). The stock solutions of MMPs/ADAMs were prepared at 200 μg/mL each, while those of the peptide substrates were prepared at concentrations of 1 mM each. The proteases and peptides were stored at -80 °C and at -20 °C, respectively, before and after immediate use. Three buffer solutions were used in this study: (1) MES buffer (containing 100 mM 2-(N-morpholino)-ethanesulfonic acid, pH 6.0); and (2) Assay buffer (pH 7.5), which was consisted of 50 mM Tris, 15 mM NaCl, 0.01% Brij-23 (w/v) and 5 μM $ZnCl_2$; and (3) Storage buffer (pH 6.5), which contained 1 mM Tris and 0.001% Brij-23 (w/v).

Instruments. Fluorescence spectra were obtained by using a luminescence spectrophotometer (LS50B, PerkinElmer, Waltham, MA, USA). Infrared (IR) spectra were recorded with an infrared spectrophotometer (NEXUS 470 FT-IR, Thermo Nicolet, Waltham, MA, USA). UV−Vis absorption spectra were collected using a UV-Vis-NIR spectrophotometer (Varian Cary 500 Scan, Agilent, Santa Clara, CA, USA).

Synthesis of Multiplex nGO-COO-Peps Biosensor. The multiplex nGO-COO-Peps sensor was fabricated by using nGO instead of GO as the starting material due to its increased edge to basal-plane ratio, thus having a larger density of carboxylate groups[37]. To further increase the percentage of the active carboxylic acid groups on the nGO surface for better coupling of the peptide substrate, we treated nGO with chloroacetic acid under strongly basic conditions to convert epoxide and hydroxyl groups to carboxylic acid moieties (Supporting Information, Figure S1). Briefly, 5 mg/mL nGO suspension was blended with 6 g NaOH and 5 g $ClCH_2COOH$, and sonicated intermittently for 2-h. The resulting solution was neutralized by HCl (1 M), and purified by repeated washing with water until the pH of the carboxylated nGO (nGO-COOH) solution reached 7.0[32]. As shown in Figure S2 (Supporting Information), the infrared spectroscopy (FT-IR) experiment with the nGO-COOH solution showed a strong absorption doublet at 1635 cm^{-1} and 1398 cm^{-1} (corresponding to the -COO symmetric and asymmetric vibrations), indicating the good conversion of carboxylate moieties -COO from nGO.

The nGO-COOH (1 mg/mL, 50 μL) prepared as above was then dispersed in 1.0 mL of MES buffer (100 mM, pH 6.0). 25 μL of 200 mM 1-ethyl-3-(-3-dimethylaminopropyl) carbodiimide hydrochloride (EDC) and 100 μL of 200 mM N-hydroxysulfosuccinimide (Sulfo-NHS) were added to the nGO-COOH suspension and sonicated for 40 min under an ice-water bath. The resulting mixture was centrifuged at 12,000 rpm for 10 min, and the supernatant was discarded. After rinsing the precipitate for three more times to remove excess EDC and Sulfo-NHS, it was dispersed in 1.0 mL water and followed by adding a 92-μL mixture of three peptide substrate solutions, which was consisted of 28 μL of Pep-MCA (1 mM), 20 μL of Pep-FAM (1 mM), and 44 μL of Pep-TAMRA (1 mM). The activated nGO-COOH / peptides mixture was stirred at

room temperature for 2 hours in darkness. Note that the volume ratio of the labeled peptide substrates (V_{MCA}: V_{FAM} : V_{TAMRA} =1.4 : 1 : 2.2) as described above was determined from the coupling reaction experiment, which involved detection of the relative reaction efficiency of a substrate peptide over the FAM-labeled peptide (E_{Sub}/E_{FAM}) as a function of their relative volume ratio (Supporting Information, Figure S3). Lastly, the product was purified by repeated centrifugation and rinsing with distilled water three times to remove the unreacted peptides, and then rinsing with 100 μL of bull serum albumin (BSA, 2 mg/mL) three times to remove non-specifically absorbed peptides on the GO surface. The final product was dispersed in the storage buffer with a final concentration of 10 μg/mL and stored in a refrigerator at 4 °C. The density of the peptide probes on nGO surface was determined using a colorimetric-based assay[33,38]. The result (0.128 μmol/mg) obtained was similar to that (0.134 μmol/mg) of the previous report by Imani et al[38].

RESULTS

Sensing Principle and Design of the Multiplex nGO-COO-Peps Biosensor. Individual biomarkers have very limited indicative value since one biomarker only represents one aspect of carcinogenesis. Hence, there is growing recognition of the need for combining multiple cancer biomarkers to improve diagnosis and/or prognosis accuracy. Furthermore, an appropriate selection of a biomarker panel can also enable discriminating between different cancer types. Unlike the conventional multiplexing sensing system, which is consisted of an array of individual selective sensors (or sensing probes) for different species, our developed multiplexed nGO-COO-Peps biosensor for protease detection was constructed by using a single graphene oxide film attached with multiple fluorophore-labeled peptide substrates having selectivities toward multiple proteases (Scheme 1a). In the absence of the target proteases (i.e., MMPs/ADAMs in this work), fluorophores are effectively quenched by nGO. However, in the presence of target MMPs/ADAMs, they will cleave the corresponding peptide substrates, thus releasing dye fragments into the solution and producing fluorescence. Since different peptides were labeled with different colored dyes, the identities of the analyte proteases could be differentiated from each other and even simultaneously determined (Scheme 1b). Given the existence of a large number of MMPs/ADAMs, selection of a subset of MMPs/ADAMs as an appropriate biomarker panel for cancer detection and diagnosis is a challenge. In general, the more biomarkers are combined, the more accurate cancer information would be obtained. However, the limited number of binding sites available on the carboxylated graphene oxide do not allow attaching a large number of different types of substrate peptides to its surface due to the concern of a low occupation ratio for each peptide species and a small signal-to-noise ratio for each peptide-protease cleavage reaction. In order to obtain the most cancer information with the fewest types of MMPs/ADAMs used in the biomarker panel, joint Shannon entropy in information theory was introduced.

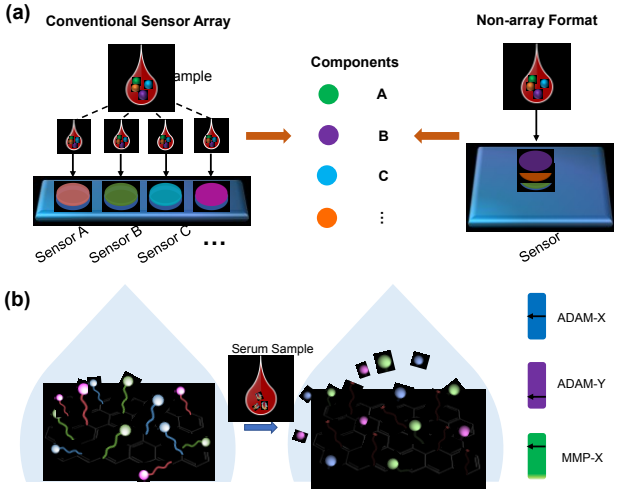

Scheme 1. (a) A cartoon display of a multiplexing sensing system in a conventional sensor array format versus the non-array format developed in this work; and (b) the schematic representation of the principle of a multiplex nGO-COO-Peps biosensor for simultaneous detection of multiple ADAMs/MMPs.

Joint entropy is a measure of the uncertainty associated with a set of the variables. Joint readings of multiple biomarkers could be described by the joint distribution of the corresponding random variables. The higher the joint entropy, the more uncertain a joint distribution is, and the more information a set of joint random variables may convey. Joint entropy is defined as follows:

$$H(V_1, \cdots, V_n) = -\sum_{v_1 \in v_1} \cdots \sum_{v_n \in v_n} P(v_1, \cdots, v_n) \log_2 [P(v_1, \cdots, v_n)] \quad (1)$$

where $P(v_1, \cdots, v_n)$ is the joint probability density function (PDF) of random variable $V_1, \cdots, V_n$ which represents the biomarkers selected, while v_i is the value space of random variable V_i. Note that, given a sample randomly selected from a population of uniformly distributed cancer type, the observed value of each biomarker could be considered as a discrete random variable which follows the Bernoulli distribution. Let $V_1, \cdots, V_n$ represent the value of n biomarkers where $V_i \sim Bernoulli(p_i), \forall\, i \in \{1, 2, \cdots, n\}$. The probability of each biomarker (summarized in Table 1) being positive could be determined, as shown in the Supporting Information, Table S2 (note that $V_1, \cdots, V_n$ are not independent with each other). As a proof-of-concept demonstration, in this work, we would design an appropriate three biomarker panel for cancer detection application. One of the main principles for biomarker design is to obtain the most cancer information with the least amounts of random variables. For this purpose, the joint entropies of all the possible combinations of three biomarkers were calculated, and the feasibility of utilizing these combinations for distinguishing human cancers was also tested by programing. The results were summarized in Table S3 and Table S4 (Supporting Information). We found that, among various combinations of three MMPs/ADAMs biomarkers, MMP-7, ADAM-8, and ADAM-9 provided the highest joint entropy of 2.66. Using this combination, 6 types of human cancers (kidney, breast, prostate, colorectal, lung,

pancreas)[5,39-41] could be identified and differentiated. However, due to the issues related to the synthesis efficiencies between nGO and substrate peptides, and the signal-to-noise ratios of the produced nGO-based fluorescent sensors in response to the target MMPs/ADAMs, ADAM-10, ADAM-17 and MMP-9 were chosen as a model three-biomarker panel to demonstrate our multiplex sensing system for simultaneous detection of multiple proteases. Note that, using this three-protease combination, a joint entropy of 2.48 was obtained, and up to 5 cancer types could be identified.

To construct a multiplex sensor for simultaneous multi-protease detection, three labeled peptide substrates containing the known sequences for ADAM-10, ADAM-17, and MMP-9, respectively, were designed according to the following principles. First, the lengths of the substrate peptides should not differ significantly, so that similar cleavage reaction rates could be obtained between them and their corresponding proteases[42]. Second, the same N-terminal amino acid sequence should be contained in each peptide in order to achieve similar reaction rates when they are coupled with graphene oxide. Third, the fluorescence spectra of the labeled dyes should have an overlap of less than 30% to avoid the self-quenching effect[43]. For these purposes, MCA, FAM, and TAMRA-labeled peptide substrates and showed three small peaks at 321 nm, 496 nm, and 562 nm, respectively (Figure 1a). These peaks were located at the similar positions as those (328 nm, 488 nm, and 556 nm) of the MCA-, FAM-, and TAMRA-labeled peptides, which were not observed in the nGO and nGO-COOH solutions. Furthermore, the fluorescence spectra of the multiplex nGO-COO-Peps sensor in the absence and presence of a mixture of ADAM-10 (100 ng/mL), ADAM-17 (100 ng/mL) and MMP-9 (100 ng/mL) proteases were recorded at $\lambda_{ex/em}$ = 321/375~450 nm, $\lambda_{ex/em}$ = 492/505~550 nm, and $\lambda_{ex/em}$ = 549/560~600 nm. Our experiments (Figure 1b) showed that, without proteases, the nGO-COO-Peps solution produced small fluorescence signals. In contrast, after addition of proteases to the solution, significantly enhanced fluorescence intensities were observed at three different wavelength ranges as mentioned above. To determine the quenching efficiencies of nGO on fluorophore-labeled peptides, the nGO-COO-Peps sensor was incubated with a mixture of ADAM-10 (500 ng/mL), ADAM-17 (500 ng/mL), and MMP-9 (500 ng/mL) for 8 hours to fully recover the fluorophores. By comparing the fluorescence intensities of nGO-COO-Peps in the absence and presence of proteases, quenching efficiencies of nGO on MCA-, FAM-, and TAMRA-labeled peptides were obtained (76.5%, 79.7%, and 65.9%, respectively). The results not

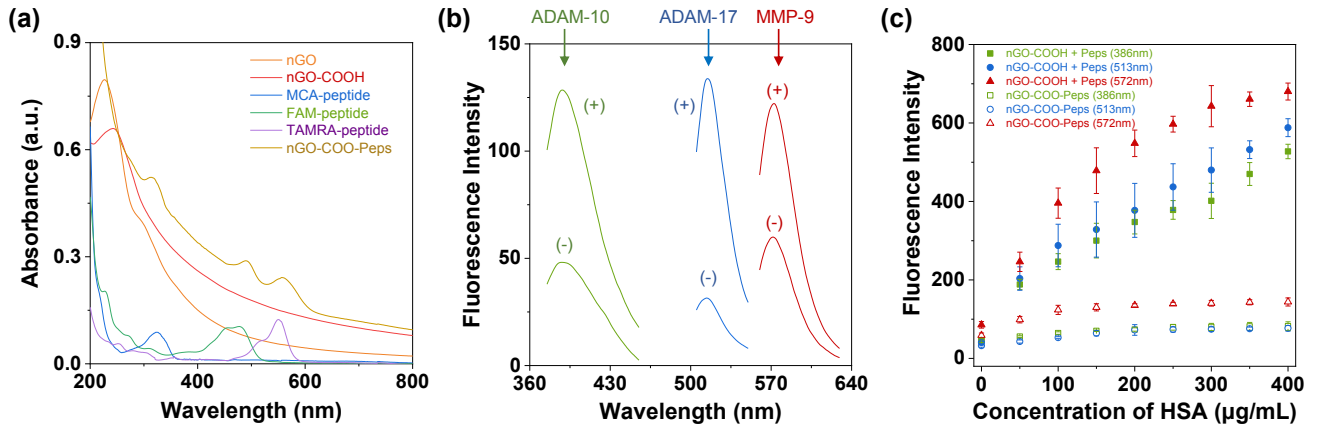

Figure 1. Characterization of the multiplex nGO-COO-Peps biosensor. (a) UV-Vis absorbance spectra of nGO, nGO-COOH, MCA-peptide, FAM-peptide, TAMRA-peptide, and multiplex nGO-COO-Peps biosensor; (b) Fluorescence spectra of the multiplex nGO-COO-Peps biosensor in the absence and presence of ADAM-10, ADAM-17, or MMP-9; (c) Effect of HSA on the nGO-COO-Peps sensor and the mixture of nGO-COOH and dye-labeled peptides. In the UV-vis experiment as shown in Fig. 1a, the concentrations of nGO, nGO-COOH and nGO-COO-Peps sensor were 10 μg/mL each, while those of the dye-labeled peptides were 10 μM each. The fluorescence measurement (displayed in Fig. 1b) was performed in the assay buffer. The concentration of the nGO-COO-Peps sensor was 5 μg/mL, while those of the proteases used were 100 ng/mL each. The mixture used in Fig. 2c was prepared by mixing 1 μg/mL nGO-COOH, 2 μM MCA-peptide, 2 μM FAM-peptide, and 2 μM TAMRA-peptide. The concentration of the nGO-COO-Peps sensor used in Fig. 2c was 5 μg/mL. Three separate experiments were performed for each sample.

(Supporting Information, Table S5), corresponding to ADAM-10, ADAM-17, and MMP-9, respectively, were synthesized and attached on the nGO surface.

nGO-COO-Peps Biosensor Characterization. The chemical structures of our designed nGO-COO-Peps sensor were confirmed by UV-Vis experiments. Similar to nGO-COOH (10 μg/mL), the nGO-COO-Peps solution (10 μg/mL) had a broad UV-vis absorption range (from ~200 nm to 800 nm). However, the nGO-COO-Peps sample had much larger absorbance values in the visible region than nGO-COOH, only indicated the existence of three dye-labeled peptides on the graphene surface, but also suggested the capability of the nGO-COO-Peps sensor for the simultaneous detection of multiple proteases. In addition, to further demonstrate that the nGO-COO-Peps sensor was constructed by covalent coupling of labeled peptides to the nGO surface instead of strong non-specific absorption (e.g., the π–π stacking and/or electrostatic interaction), the effect of human serum albumin (HSA, an abundant serum protein) on the sensor stability was investigated. Note that as dis-

cussed in our previous study[32,44], fluorescence can be quenched by both the covalent conjugation and strong non-specific absorption between nGO and labeled peptides. However, non-specific absorption of labeled peptides on the nGO surface is unstable and can be easily disturbed when other similar molecules, especially proteins, competitively bind to nGO. For this purpose, the nGO-COO-Peps sensor and the mixture of nGO-COOH and dye-labeled peptides (Pep-FAM, Pep-MCA, and Pep-TAMRA) were incubated with a series of HSA with different concentrations for 30 min at room temperature, followed by measuring their fluorescence intensities. As shown in Figure 1c, with an increase in the concentration of added HSA, the fluorescence intensities of the nGO-COOH/Pep-FAM/Pep-MCA/Pep-TAMRA mixture increased drastically at three different wavelengths, while those of the nGO-COO-Peps sensor showed only a slight increase even when the concentration of HSA reached as high as 400 μg/mL. Taken together, the combined results supported our successful construction of nGO-COO-Peps conjugate.

Optimization of Experimental Conditions. Incubation time is a well-known factor that influences enzyme-substrate cleavage reactions. However, it should be noted that, the product formation rate of proteolytic reaction is not a simple linear function of the incubation time because all proteins lose catalytic activity with time due to denaturation. Furthermore, different proteases may have different kinetic and thermodynamic parameters as well as catalytic efficiencies. To find an optimal reaction time for rapid, sensitive, and simultaneous detection of multiple MMPs/ADAMs, the effects of incubation time on ADAM-10, ADAM-17, and MMP-9's cleavage by our developed nGO-COO-Peps sensor was investigated. The results (plots of the increase in the fluorescence intensity of the nGO-COO-Peps solution in the absence and presence of proteases, ΔF, as a function of incubation time) were summarized in Figure 2a. We found that MMP-9 showed a relatively low reaction rate compared with ADAM-10 and ADAM-17. The reaction rates of these three proteases were in the order of $\upsilon_{ADAM\text{-}17} > \upsilon_{ADAM\text{-}10} > \upsilon_{MMP\text{-}9}$ (note that a larger change in the fluorescence intensity of the nGO-COO-Peps solution in the absence and presence of proteases represents a larger enzymatic reaction rate). To be more specific, the reaction rate for ADAM-17 increased with an increase in the reaction time until 90 minutes, after which the fluorescence signal began to saturate. In sharp contrast, there was no significant fluorescence intensity enhancement for MMP-9 until 40 min incubation time. To achieve both rapid and sensitive detection of these three proteases simultaneously, 80 min was chosen as the optimum reaction time and used in all the subsequent experiments.

In addition to the incubation time, it is well known that solution pH would affect the enzyme activity and hence have a significant influence on the performance of the nGO-COO-Peps biosensor. Furthermore, a change in the solution pH might lead to a change in the dominant species of the fluorophore[44], which also affects the fluorescence intensity of the sensor. To find an optimal solution pH, detection of ADAM-10, ADAM-17 and MMP-9 was further carried out in a series of solutions with different pH values ranging from 3.0 to 10.0. The fluorescence efficiencies of each protease (defined as the change in the fluorescent intensity before and after proteolytic reaction divided by the fluorescent signal before proteolytic reaction) under different pH conditions were summarized in Figure 2b. It was apparent that the fluorescence efficiency and hence the activity of ADAM-17 was high in a pH range from 5 to 7.5, while high activity for ADAM-10 and MMP-9 was observed from pH 4.5 to pH 8.0, and from pH 7.5 to pH 9.0, respectively. Taken together, for highly sensitive simultaneous detection of ADAM-10, ADAM-17 and MMP-9, pH 7.5 was deemed as an appropriate solution pH and used in the remaining experiments. It is worth mentioning that, unlike MMP-9, whose low proteolytical efficiency was due to its low kinetic effect parameters[45], the reason why ADAM-10 had a lower reaction rate and proteolytical efficiency than that of ADAM-17 might be attributed to the lysine motif in the sequence of the substrate peptide Pep-MCA. The amine groups on the sidechain may result in uncontrolled peptide orientations when Pep-MCA was attached to the nGO surface, thus affecting quenching and proteolytic efficiency[46].

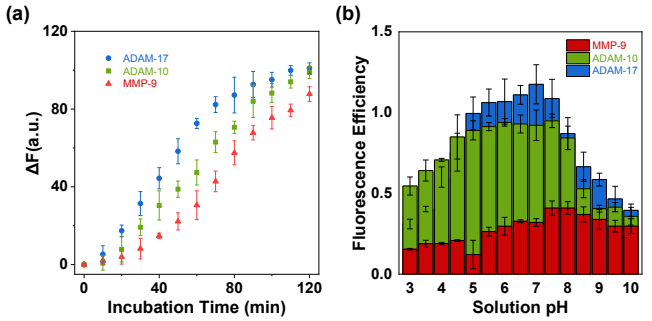

Figure 2. Optimization of experimental conditions. (a) The effects of incubation time on ADAM-10, ADAM-17, and MMP-9's cleavage by the nGO-COO-Peps sensor. (b) The effect of solution pH on the performance of nGO-COO-Peps. The experiments were performed in the presence of 1 μg/mL nGO-COO-Peps and 100 ng/mL of ADAM-10, ADAM-17, or MMP-9. The fluorescence intensities were collected at $\lambda_{ex/em}$ = 321/386, 492/513, 549/572 nm, respectively. Four separate experiments were performed for each sample.

In the previous section "nGO-COO-Peps Biosensor Characterization", we have shown that the presence of HSA in the sample solution would affect the fluorescence signal of the nGO-COO-Peps sensor due to its competitive binding to the GO surface. Briefly, with an increase in the concentration of added HSA, the background fluorescence intensity of our sensor suspension increased slightly until the concentration of HSA reached 150 μg/mL, and then began to saturate (Figure 1c and Supporting Information, Figure S4). Therefore, in order to minimize the matrix effect for serum sample analysis, 400 μg/mL HSA was added to the assay buffer in advance to saturate the background fluorescence signal. Furthermore, as an added importance, with serum albumin in the assay buffer, the dispersivity of the nGO-COO-Peps sensor in serum could be improved (note that using serum albumin as a dispersing agent to stabilize GO-based sensor has been reported by Chang et al[47]).

Sensor Sensitivity and Selectivity. Under the optimized experimental conditions (i.e., pH 7.5, 80 min reaction time, and 37 °C incubation temperature), dose response curves for the three proteases were constructed by monitoring the fluorescence signal of the nGO-COO-Peps biosensor in the presence of ADAM-10, ADAM-17 or MMP-9 at various concentrations, ranging from 10 ng/mL to 200 ng/mL. As shown in Figure 3, the fluorescence intensity of the sensor solution linearly increased with the protease concentration in three different wavelength regions, suggesting that the three peptide substrates conjugated on the GO surface could efficiently interact with their corresponding proteases. The limits of detection (LOD) of our sensor were 5.91 ng/mL for ADAM-10 (equivalent to 113.7 pM), 1.54 ng/mL for ADAM-17 (equivalent to 29.6 pM), and 8.23 ng/mL for MMP-9 (equivalent to 107.3 pM), respectively (note that LOD was defined as the concentration of protease corresponding to three times the standard deviation of the blank signal). As far as we are aware, such detection limits are sufficient to analyze these three MMPs/ADAMs in clinical samples (note that their concentrations in the blood and urine samples of healthy people are generally on the order of tens to hundreds of ng/mL[48-51]).

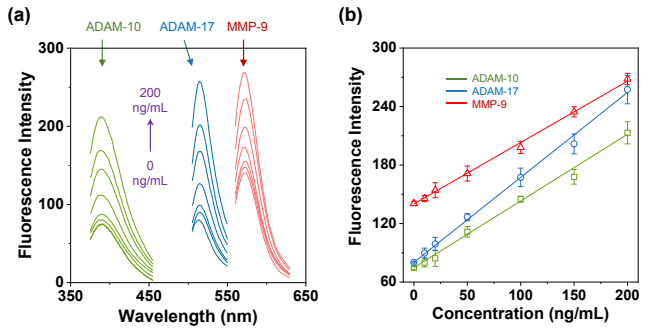

Figure 3. Sensitivity of the nGO-COO-Peps sensor. (a) Fluorescence spectra of nGO-COO-Peps in the presence of ADAM-10, ADAM-17, and MMP-9 at various concentrations; and (b) plot of fluorescence intensity versus protease concentration. Experiments were performed by incubating nGO-COO-Peps (1 μg/mL, in assay buffer, pH 7.5) and ADAM-10, ADAM-17, or MMP-9 with concentrations ranging from 0 to 200 ng/mL for 80 min at 37 °C, followed by measuring their fluorescence intensities at room temperature. Four separate experiments were performed for each sample.

To examine the sensor selectivity, we studied the interactions between two additional ADAMs (i.e., ADAM-8 and ADAM-9) and the nGO-COO-Peps biosensor. Note that ADAM-8 and ADAM-9, which are also important cancer biomarkers, have similar structures to the three proteases under investigation and hence could be utilized as appropriate potential interfering species to examine the selectivity of the nGO-COO-Peps sensor. Our experimental results (Figure 4) showed that all the non-target proteases produced significantly smaller fluorescence signals than the target analytes. In addition, the interaction between the mixture of ADAM-10, ADAM-17 and MMP-9 and the nGO-COO-Peps sensor was also examined. We found that the fluorescence intensities of the individual ADAM-10, ADAM-17 or MMP-9 standards were not significantly different from those of their corresponding mixture solutions. Taken together, the combined results suggest that our developed nGO-COO-Peps sensor was highly selective (other proteases would not interfere with the target MMP/ADAM detection significantly).

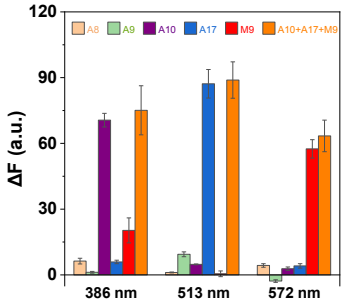

Figure 4. Selectivity of the nGO-COO-Peps sensor. The experiments were performed in the presence of individual standards of ADAM-8, ADAM-9, ADAM-10, ADAM-17, and MMP-9 as well as the mixture of ADAM-10, ADAM-17, and MMP-9 at $\lambda_{ex/em}$ = 321/386 nm, $\lambda_{ex/em}$ = 492/513 nm, and $\lambda_{ex/em}$ = 549/572 nm. The fluorescence intensity values were background corrected, which were obtained by subtracting the blank fluorescence intensity from that of the analyte species. The protease concentrations were 100 ng/mL each. Four separate experiments were performed for each sample.

Simulated Serum Sample Analysis. As a proof-of-concept purpose, we used the developed multiplex nGO-COO-Peps sensor to profile ADAM-9, ADAM-17, and MMP-9 in four simulated serum samples. These simulated serum samples were obtained by spiking these three proteases into the human serum with their concentrations / activities similar to those found in cancer patients. For example, the serum samples of gastric cancer patients usually contained ~ tens to hundreds nanograms per milliliter of ADAM-10 and ADAM-17, while similar levels of ADAM-10 and MMP-9, ADAM-17 and MMP-9, as well as ADAM-10, ADAM-17 and MMP-9 were found in the serum samples of lung cancer, breast cancer and prostate cancer, and male colorectal cancer patients[49,52,53], respectively. Experimental results (summarized in Table 1) showed that these simulated serum samples could be accurately quantitated with recoveries ranging from 94% to 121%, supporting the feasibility of our developed multiplex nGO-COO-Peps sensor for potential clinical applications.

Table 1. Recovery of ADAM-10, ADAM-17, and MMP-9 from human serum by use of the multiplex nGO-COO-Peps sensor. Each value represents the mean of three replicate analyses ± one standard deviation.

Sample	Theoretical value (ng/mL)		Experimental value ± SD (ng/mL)	
ADAM-10 + ADAM-17	ADAM-10	40	ADAM-10	38.9 ± 2.7
	ADAM-17	20	ADAM-17	20.8 ± 1.3
	MMP-9	0	MMP-9	ND
ADAM-10 + MMP-9	ADAM-10	40	ADAM-10	42.5 ± 5.6
	ADAM-17	0	ADAM-17	ND
	MMP-9	60	MMP-9	56.3 ± 6.7
ADAM-17 + MMP-9	ADAM-10	0	ADAM-10	ND
	ADAM-17	20	ADAM-17	23.5 ± 3.7

	MMP-9	60	MMP-9	52.5 ± 4.8
ADAM-10 + ADAM-17 + MMP-9	ADAM-10	40	ADAM-10	47.2 ± 8.1
	ADAM-17	20	ADAM-17	24.3 ± 4.8
	MMP-9	60	MMP-9	64.9 ± 6.2

* ND: not detected.

DISCUSSION

Using a combination of multiple biomarkers instead of a single biomarker as a predictive and diagnosis indicator can not only provide more accurate cancer diagnosis, but also enable discrimination between different cancer types. By taking advantage of our developed graphene oxide-based multiplex biosensor, a panel of MMP-9, ADAM-10 and ADAM-17 biomarkers could be utilized to diagnose up to 5 types of cancers, including breast, gastric, lung, colorectal and prostate. Clearly, other types of cancers can be detected by changing the components in the biomarker panel (refer to Supporting Information, Table S4). Furthermore, if the reaction efficiency, occupation ratio and signal efficiency of the nGO-COO-Peps sensor could be enhanced dramatically, we can attach additional MMPs/ADAMs to the GO surface. Thus, by increasing the number of biomarkers used in the diagnosis panel, we can further improve the accuracy of cancer detection, and also increase the number of cancer types to be analyzed/differentiated. For instance, use of four instead of three ADAMs/MMPs as a biomarker panel is able to distinguish up to 9 rather than 6 cancer types under the optimal condition. Note that, although the activity of each MMP/ADAM component in the sample could be measured by using an array of individual selective sensors (i.e., detection of one protease at a time), detection of the activities of multiple MMPs/ADAMs in a single assay has many advantages over single measure systems, including reduced assay costs, improved turnaround time, reduced sample/reagent volume, high-throughput screening, and decrease in errors between inter-sampling.

In this study, we took advantage of the joint entropy to select certain combinations of biomarkers for cancer detection and diagnosis. As stated in the previous sections, joint entropy is mainly used to describe the uncertainty of a joint distribution. However, there may be some discrepancy between the uncertainty joint entropy described and the objective of the biomarker panel design. Joint entropy considers not only the number of clusters that a combination of biomarkers could distinguish but also the distribution of cancer types in each cluster. However, from the biomarker panel design perspective, the distribution within each cluster perhaps does not make any difference. Second, since external factors such as gender, age, etc. play an important role in cancer diagnosis, designing an entropy that incorporate the influence of these factors will be much more efficient and valuable. The last but not the least, the accuracy we discussed in this work should also include the accuracy of each biomarker component. Some biomarkers may provide more accurate, reproducible, and reliable cancer diagnosis than others. The reliability of different biomarkers could be described as the variance which could be evaluated with repeated experiments. Clearly, when selecting a combination of biomarkers as the diagnosis panel, more reliable biomarkers should be considered.

It should be noted that, program computing plays a promising role in the entropy calculation and test result evaluation process. In this work, we evaluated the possible combinations of 15 MMPs/ADAMs since they were frequently reported so far with elevated activity levels identified in clinical samples from cancer patients. There are $\binom{15}{3} = 455$ possible combinations if we randomly select three from fifteen biomarkers. Furthermore, when they are used to evaluate 11 cancer types, around 5005 cases need to be analyzed, which may take hours to accomplish if the operation is manually performed by using human labor. With the development of new cancer biomarkers such as human kallikrein-related peptidase (KLK)[54,55], the evaluation workload will increase exponentially. Hence, it is desirable to take advantage of program computing to find the optimal solution. In the future and in practice, human intervention should be rarely required in the evaluation and analysis of the biomarker results, and the process should be automated with program computing, which could not only reduce the error percentage but also increase efficiency.

CONCLUSION

In summary, by taking advantage of graphene oxide, we successfully designed and developed a multiplexed fluorescence-based sensing system in a non-array format for simultaneous detection of the activities of multiple MMPs/ADAMs. The designed nGO-COO-Peps sensor was rapid, sensitive and selective. It was also utilized for the successful profiling of ADAMs/MMPs in simulated serum samples. Under the assistance of joint entropy and programming, the three biomarkers (MMP-9, ADAM-10 and ADAM-17) used in this work can serve as a biomarker panel for diagnosis of up to 5 cancer types, including breast, gastric, lung, colorectal and prostate. It could be visualized that other types of cancers can also be detected by changing the components in the biomarker panel. Our developed GO-based multiplex sensing platform could find useful application in early cancer detection and diagnosis.

ASSOCIATE CONTENT

Supporting Information

Additional table and figures, including type of cancer and its corresponding MMPs/ADAMs detected in tissue/ body fluid, the probability density function (PDF) of individual protease biomarkers, the joint distribution of MMP-9, ADAM-10 and ADAM-17, the top 24 list of joint entropies among the various combinations of three ADAMs/MMPs and their corresponding potentially distinguishable cancer types, the designed substrate peptide sequences of proteases, the synthetic route for constructing the GO-based multiplex biosensor, FT-IR spectra of nGO and nGO-COOH, investigation of the volume ratio of the labeled peptide substrates for efficient synthesis of the multiplex nGO-

COO-Peps biosensor, and effect of HSA on the nGO-COO-Peps sensor.

AUTHOR INFORMATION

Corresponding author

*Tel: 312-567-8922. Fax: 312-567-3494.
E-mail: xguan5@iit.edu and wangliang83@cigit.ac.cn

Notes

The authors declare no competing financial interests.

ACKNOWLEDGMENTS

This work was financially supported by the National Institutes of Health (2R15GM110632-02) and National Science Foundation (1708596)

REFERENCE

(1) Sidransky, D. *Nat. Rev. Cancer* **2002**, *2*, 210-219.
(2) Peveler, W. J.; Yazdani, M.; Rotello, V. M. *ACS Sensors* **2016**, *1*, 1282-1285.
(3) Albert, K. J.; Lewis, N. S.; Schauer, C. L.; Sotzing, G. A.; Stitzel, S. E.; Vaid, T. P.; Walt, D. R. *Chem. Rev. (Washington, DC, U. S.)* **2000**, *100*, 2595-2626.
(4) Turk, B. E.; Huang, L. L.; Piro, E. T.; Cantley, L. C. *Nat. Biotechnol.* **2001**, *19*, 661.
(5) Roy, R.; Yang, J.; Moses, M. A. *Journal of Clinical Oncology* **2009**, *27*, 5287-5297.
(6) Bode, W. *Biochem. Soc. Symp.* **2003**, *70*, 1.
(7) Roy, R.; Zurakowski, D.; Pories, S.; Moses, M. A.; Moss, M. L. *Clin. Biochem.* **2011**, *44*, 1434-1439.
(8) Schulz, R. *Annu. Rev. Pharmacol. Toxicol.* **2007**, *47*, 211-242.
(9) Lin, Y.-H.; Lin, L.-Y.; Wu, Y.-W.; Chien, K.-L.; Lee, C.-M.; Hsu, R.-B.; Chao, C.-L.; Wang, S.-S.; Hsein, Y.-C.; Liao, L.-C.; Ho, Y.-L.; Chen, M.-F. *Clin. Chim. Acta* **2009**, *409*, 96-99.
(10) Moss, M. L.; Rasmussen, F. H. *Anal. Biochem.* **2007**, *366*, 144-148.
(11) Stone, A. L.; Kroeger, M.; Sang, Q. X. A. *J. Protein Chem.* **1999**, *18*, 447-465.
(12) Edwards, D. R.; Handsley, M. M.; Pennington, C. J. *Molecular Aspects of Medicine* **2008**, *29*, 258-289.
(13) Murphy, G. *Nat. Rev. Cancer* **2008**, *8*, 932.
(14) Overall, C. M.; Kleifeld, O. *Nat. Rev. Cancer* **2006**, *6*, 227.
(15) Brinckerhoff, C. E.; Matrisian, L. M. *Nat. Rev. Mol. Cell Biol.* **2002**, *3*, 207.
(16) Egeblad, M.; Werb, Z. *Nat. Rev. Cancer* **2002**, *2*, 161.
(17) Bachmeier, B. E.; Iancu, C. M.; Jochum, M.; Nerlich, A. G. *Expert Review of Anticancer Therapy* **2005**, *5*, 149-163.
(18) Curran, S.; Murray, G. I. *The Journal of Pathology* **1999**, *189*, 300-308.
(19) Pories, S. E.; Zurakowski, D.; Roy, R.; Lamb, C. C.; Raza, S.; Exarhopoulos, A.; Scheib, R. G.; Schumer, S.; Lenahan, C.; Borges, V.; Louis, G. W.; Anand, A.; Isakovich, N.; Hirshfield-Bartek, J.; Wewer, U.; Lotz, M. M.; Moses, M. A. *Cancer Epidemiology Biomarkers & Prevention* **2008**, *17*, 1034.
(20) Roy, R.; Wewer, U. M.; Zurakowski, D.; Pories, S. E.; Moses, M. A. *J. Biol. Chem.* **2004**, *279*, 51323-51330.
(21) Robins, H. I.; O'Neill, A.; Gilbert, M.; Olsen, M.; Sapiente, R.; Berkey, B.; Mehta, M. *Cancer chemotherapy and pharmacology* **2008**, *62*, 227-233.
(22) Sideras, K.; Schaefer, P. L.; Okuno, S. H.; Sloan, J. A.; Kutteh, L.; Fitch, T. R.; Dakhil, S. R.; Levitt, R.; Alberts, S. R.; Morton, R. F.; Rowland, K. M.; Novotny, P. J.; Loprinzi, C. L. *Mayo Clinic Proceedings* **2006**, *81*, 758-767.
(23) Loprinzi, C. L.; Levitt, R.; Barton, D. L.; Sloan, J. A.; Atherton, P. J.; Smith, D. J.; Dakhil, S. R.; Moore, D. F.; Krook, J. E.; Rowland, K. M.; Mazurczak, M. A.; Berg, A. R.; Kim, G. P. *Cancer* **2005**, *104*, 176-182.
(24) Roy, R.; Yang, J.; Moses, M. A. *Journal of Clinical Oncology* **2009**, *27*, 5287-5297.
(25) Trad, A.; Hedemann, N.; Shomali, M.; Pawlak, V.; Grötzinger, J.; Lorenzen, I. *J. Immunol. Methods* **2011**, *371*, 91-96.
(26) Toth, M.; Sohail, A.; Fridman, R. In *Metastasis Research Protocols*, Dwek, M.; Brooks, S. A.; Schumacher, U., Eds.; Humana Press: Totowa, NJ, 2012, pp 121-135.
(27) Bolduc, O. R.; Pelletier, J. N.; Masson, J.-F. *Anal. Chem.* **2010**, *82*, 3699-3706.
(28) Shetty, V.; Spellman, D. S.; Neubert, T. A. *J. Am. Soc. Mass Spectrom.* **2007**, *18*, 1544-1551.
(29) Wei, Q.; Seward, G. K.; Hill, P. A.; Patton, B.; Dimitrov, I. E.; Kuzma, N. N.; Dmochowski, I. J. *J. Am. Chem. Soc.* **2006**, *128*, 13274-13283.
(30) Liu, G.; Wang, J.; Wunschel, D. S.; Lin, Y. *J. Am. Chem. Soc.* **2006**, *128*, 12382-12383.
(31) Chen, X.; Zhang, Y.; Mohammadi Roozbahani, G.; Guan, X. *ACS Applied Bio Materials* **2019**, *2*, 504-509.
(32) Zhang, Y.; Chen, X.; Roozbahani, G. M.; Guan, X. *Anal. Bioanal. Chem.* **2018**, *410*, 6177-6185.
(33) Wu, Y.; Wang, A.; Ding, X.; Xu, F.-J. *ACS Appl. Mater. Interfaces* **2017**, *9*, 127-135.
(34) Wu, Y.; Nizam, M. N.; Ding, X.; Xu, F.-J. *ACS Biomaterials Science & Engineering* **2018**, *4*, 2018-2025.
(35) Kim, J.; Cote, L. J.; Kim, F.; Yuan, W.; Shull, K. R.; Huang, J. *J. Am. Chem. Soc.* **2010**, *132*, 8180-8186.
(36) Swathi, R. S.; Sebastian, K. L. *The Journal of Chemical Physics* **2009**, *130*, 086101.
(37) Chou, S. S.; De, M.; Luo, J.; Rotello, V. M.; Huang, J.; Dravid, V. P. *J. Am. Chem. Soc.* **2012**, *134*, 16725-16733.
(38) Imani, R.; Emami, S. H.; Faghihi, S. *Phys. Chem. Chem. Phys.* **2015**, *17*, 6328-6339.
(39) Kuhlmann, K. F. D.; van Till, J. W. O.; Boermeester, M. A.; de Reuver, P. R.; Tzvetanova, I. D.; Offerhaus, G. J. A.; ten Kate, F. J. W.; Busch, O. R. C.; van Gulik, T. M.; Gouma, D. J.; Crawford, H. C. *Cancer epidemiology, biomarkers & prevention : a publication of the American Association for Cancer Research, cosponsored by the American Society of Preventive Oncology* **2007**, *16*, 886-891.
(40) Grützmann, R.; Lüttges, J.; Sipos, B.; Ammerpohl, O.; Dobrowolski, F.; Alldinger, I.; Kersting, S.; Ockert, D.; Koch, R.; Kalthoff, H.; Schackert, H. K.; Saeger, H. D.; Klöppel, G.; Pilarsky, C. *Br. J. Cancer* **2004**, *90*, 1053.
(41) Mochizuki, S.; Okada, Y. *Cancer Sci.* **2007**, *98*, 621-628.
(42) Silvestre, M. P. C. *Food Chem.* **1997**, *60*, 263-271.
(43) Sekar, R. B.; Periasamy, A. *The Journal of cell biology* **2003**, *160*, 629-633.
(44) Zhang, Y.; Chen, X.; Roozbahani, G. M.; Guan, X. *Analyst* **2019**, *144*, 1825-1830.
(45) Kridel, S. J.; Chen, E.; Kotra, L. P.; Howard, E. W.; Mobashery, S.; Smith, J. W. *J. Biol. Chem.* **2001**, *276*, 20572-20578.
(46) Spicer, C. D.; Jumeaux, C.; Gupta, B.; Stevens, M. M. *Chem. Soc. Rev.* **2018**, *47*, 3574-3620.
(47) Chang, H. Y.; Lin, C.-y.; Chang, C.; Teng, H.; Campagnola, P.; Chen, S. *Optical Materials Express* **2016**, *6*, 3193-3201.
(48) Thrailkill, K. M.; Bunn, R. C.; Moreau, C. S.; Cockrell, G. E.; Simpson, P. M.; Coleman, H. N.; Frindik, J. P.; Kemp, S. F.; Fowlkes, J. L. *Diabetes Care* **2007**, *30*, 2321.
(49) Walkiewicz, K.; Nowakowska-Zajdel, E.; Strzelczyk, J.; Dzięgielewska-Gęsiak, S.; Muc-Wierzgoń, M. *Journal of biological regulators and homeostatic agents* **2017**, *31*, 929-934.
(50) Szarvas, T.; Singer, B. B.; Becker, M.; vom Dorp, F.; Jäger, T.; Szendrői, A.; Riesz, P.; Romics, I.; Rübben, H.; Ergün, S. *BJU International* **2011**, *107*, 1069-1073.
(51) INCORVAIA, L.; BADALAMENTI, G.; RINI, G.; ARCARA, C.; FRICANO, S.; SFERRAZZA, C.; DI TRAPANI, D.; GEBBIA, N.; LETO, G. *Anticancer Res.* **2007**, *27*, 1519-1525.
(52) Riedel, F.; Gotte, K.; Schwalb, J.; Hormann, K. *Anticancer Res.* **2000**, *20*, 3045-3049.
(53) Paweł, K.; Katarzyna, W.; Joanna, S.; Sylwia, D.-G.; Dariusz, W.; Angelika, C.; Malgorzata, M.-W.; Ewa Nowakowska, Z. *Journal of Gastrointestinal & Digestive System* **2016**, *6*, 55.
(54) Dorn, J.; Magdolen, V.; Gkazepis, A.; Gerte, T.; Harlozinska, A.; Sedlaczek, P.; Diamandis, E. P.; Schuster, T.; Harbeck, N.; Kiechle, M.; Schmitt, M. *Annals of Oncology* **2011**, *22*, 1783-1790.
(55) Kryza, T.; Silva, M. L.; Loessner, D.; Heuzé-Vourc'h, N.; Clements, J. A. *Biochimie* **2016**, *122*, 283-299.

Table 1. Recovery of ADAM-10, ADAM-17, and MMP-9 from human serum by use of the multiplex nGO-COO-Peps sensor. Each value represents the mean of three replicate analyses ± one standard deviation.

Sample	Theoretical value (ng/mL)		Experimental value ± SD (ng/mL)	
ADAM-10 + ADAM-17	ADAM-10	40	ADAM-10	38.9 ± 2.7
	ADAM-17	20	ADAM-17	20.8 ± 1.3
	MMP-9	0	MMP-9	ND
ADAM-10 + MMP-9	ADAM-10	40	ADAM-10	42.5 ± 5.6
	ADAM-17	0	ADAM-17	ND
	MMP-9	60	MMP-9	56.3 ± 6.7
ADAM-17 + MMP-9	ADAM-10	0	ADAM-10	ND
	ADAM-17	20	ADAM-17	23.5 ± 3.7
	MMP-9	60	MMP-9	52.5 ± 4.8
ADAM-10 + ADAM-17 + MMP-9	ADAM-10	40	ADAM-10	47.2 ± 8.1
	ADAM-17	20	ADAM-17	24.3 ± 4.8
	MMP-9	60	MMP-9	64.9 ± 6.2

* ND: not detected.

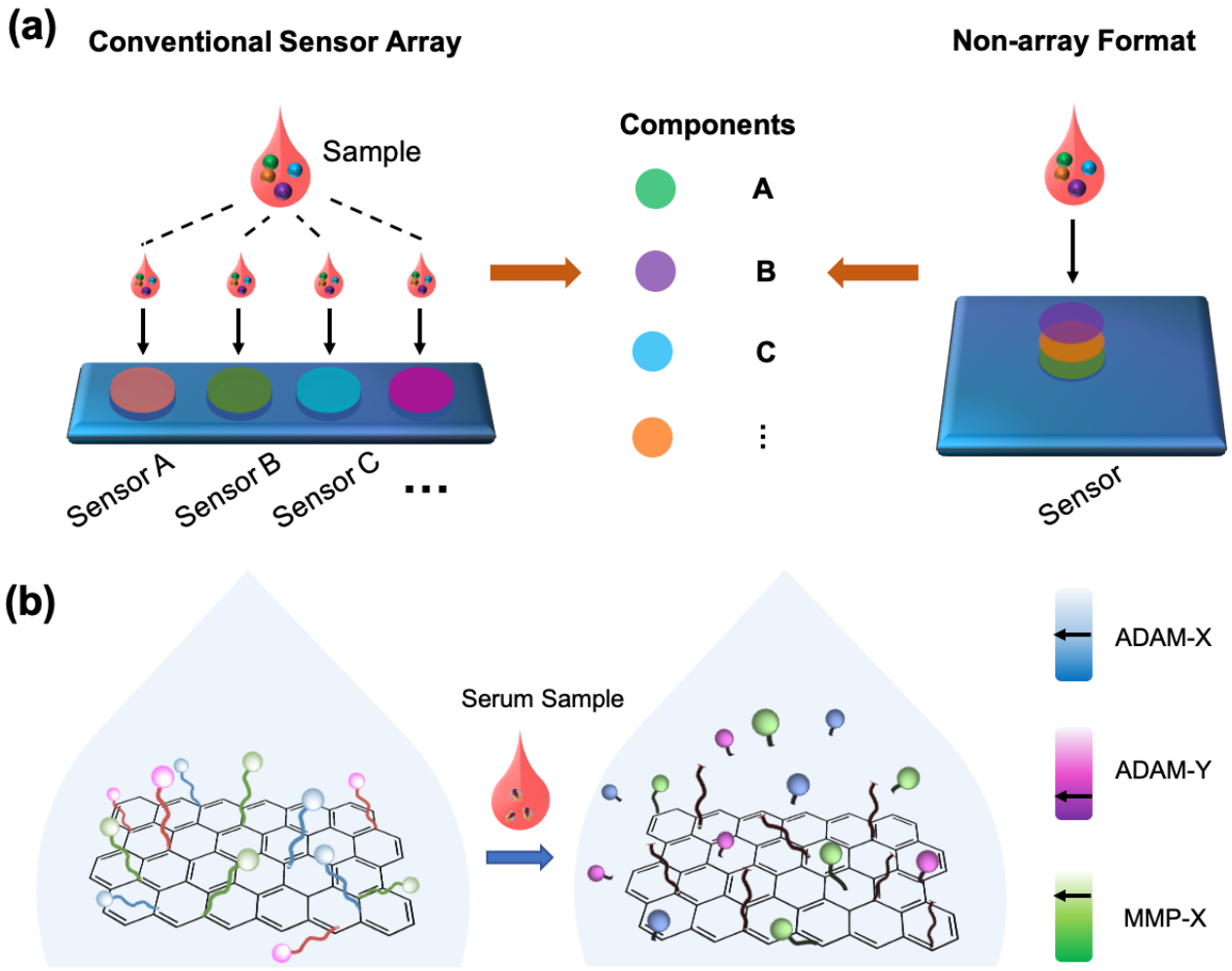

Scheme 1. (a) A cartoon display of a multiplexing sensing system in a conventional sensor array format versus the non-array format developed in this work; and (b) the schematic representation of the principle of a multiplex nGO-COO-Peps biosensor for simultaneous detection of multiple ADAMs/MMPs.

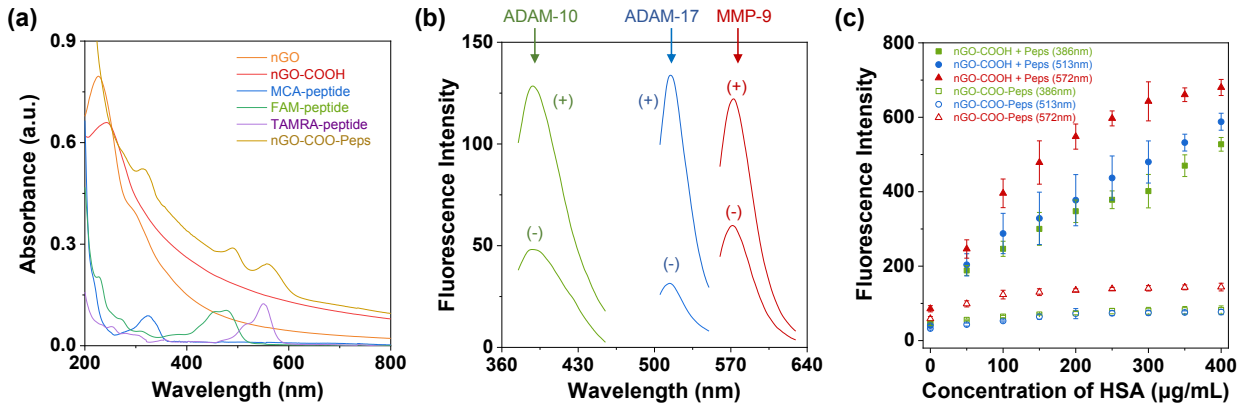

Figure 1. Characterization of the multiplex nGO-COO-Peps biosensor. (a) UV-Vis absorbance spectra of nGO, nGO-COOH, MCA-peptide, FAM-peptide, TAMRA-peptide, and multiplex nGO-COO-Peps biosensor; (b) Fluorescence spectra of the multiplex nGO-COO-Peps biosensor in the absence and presence of ADAM-10, ADAM-17, or MMP-9; (c) Effect of HSA on the nGO-COO-Peps sensor and the mixture of nGO-COOH and dye-labeled peptides. In the UV-vis experiment as shown in Fig. 1a, the concentrations of nGO, nGO-COOH and nGO-COO-Peps sensor were 10 μg/mL each, while those of the dye-labeled peptides were 10 μM each. The fluorescence measurement (displayed in Fig. 1b) was performed in the assay buffer. The concentration of the nGO-COO-Peps sensor was 5 μg/mL, while those of the proteases used were 100 ng/mL each. The mixture used in Fig. 1c was prepared by mixing 1 μg/mL nGO-COOH, 2 μM MCA-peptide, 2 μM FAM-peptide, and 2 μM TAMRA-peptide. The concentration of the nGO-COO-Peps sensor used in Fig. 1c was 5 μg/mL. Three separate experiments were performed for each sample.

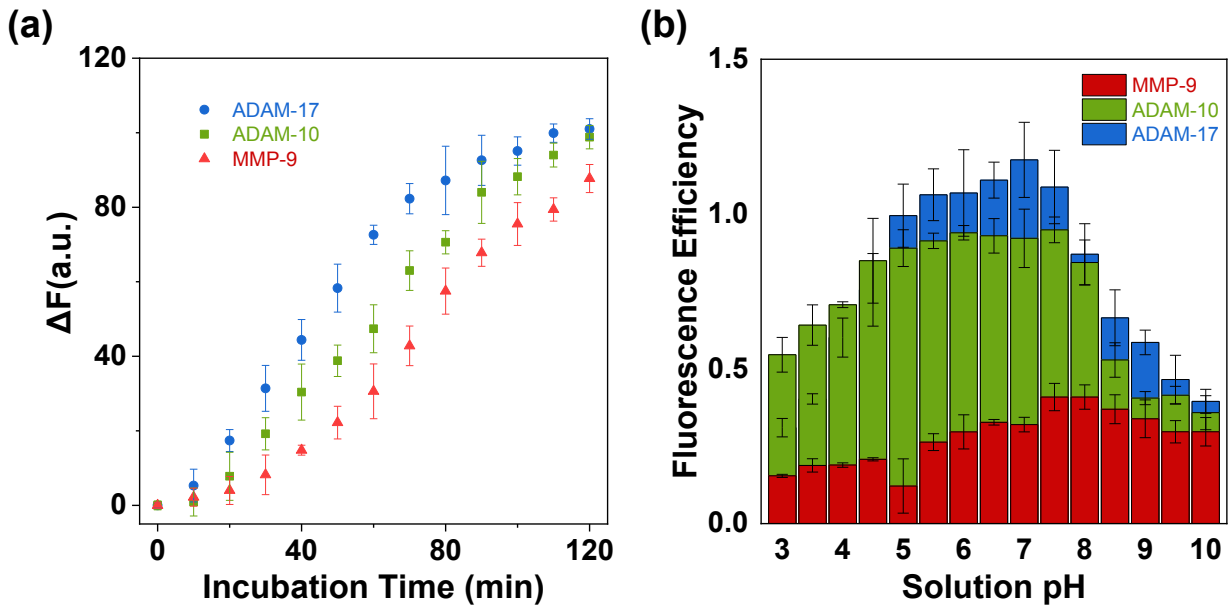

Figure 2. Optimization of experimental conditions. (a) The effects of incubation time on ADAM-10, ADAM-17, and MMP-9's cleavage by the nGO-COO-Peps sensor. (b) The effect of solution pH on the performance of nGO-COO-Peps. The experiments were performed in the presence of 1 μg/mL nGO-COO-Peps and 100 ng/mL of ADAM-10, ADAM-17, or MMP-9. The fluorescence intensities were collected at $\lambda_{ex/em}$ = 321/386, 492/513, 549/572 nm, respectively. Four separate experiments were performed for each sample.

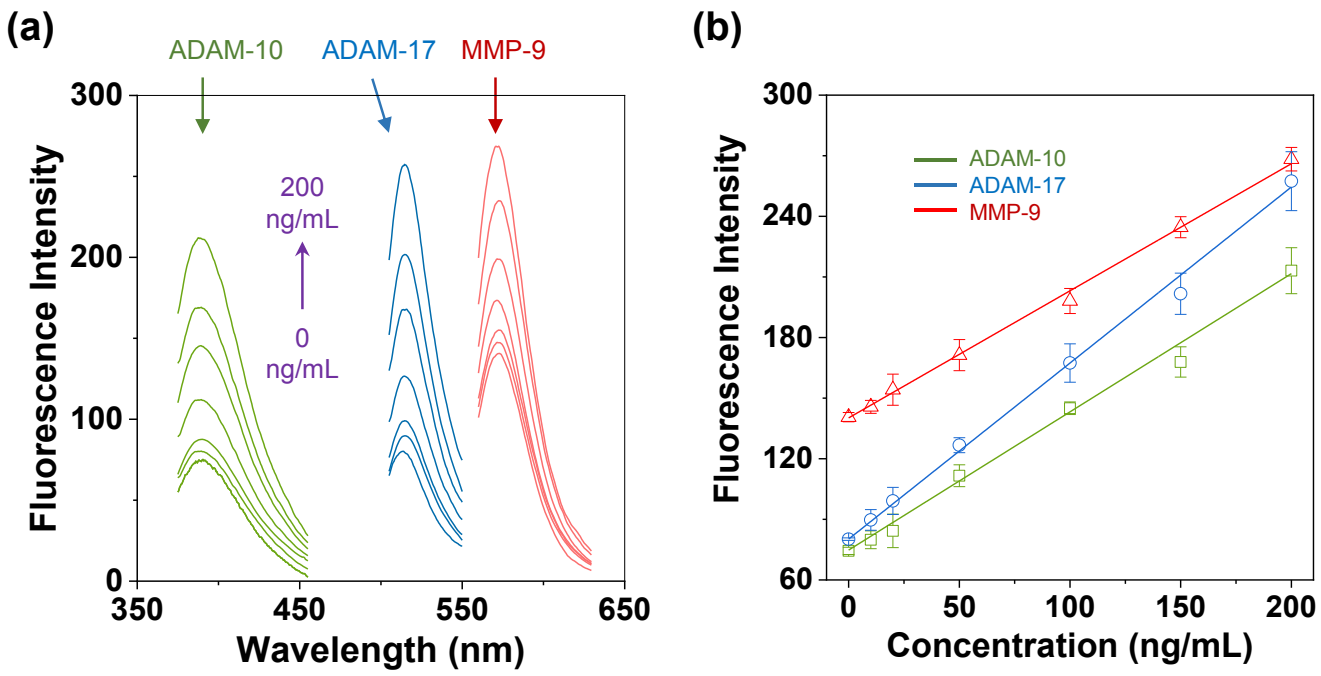

Figure 3. Sensitivity of the nGO-COO-Peps sensor. (a) Fluorescence spectra of nGO-COO-Peps in the presence of ADAM-10, ADAM-17, and MMP-9 at various concentrations; and (b) plot of fluorescence intensity versus protease concentration. Experiments were performed by incubating nGO-COO-Peps (1 μg/mL, in assay buffer, pH 7.5) and ADAM-10, ADAM-17, or MMP-9 with concentrations ranging from 0 to 200 ng/mL for 80 min at 37 °C, followed by measuring their fluorescence intensities at room temperature. Four separate experiments were performed for each sample.

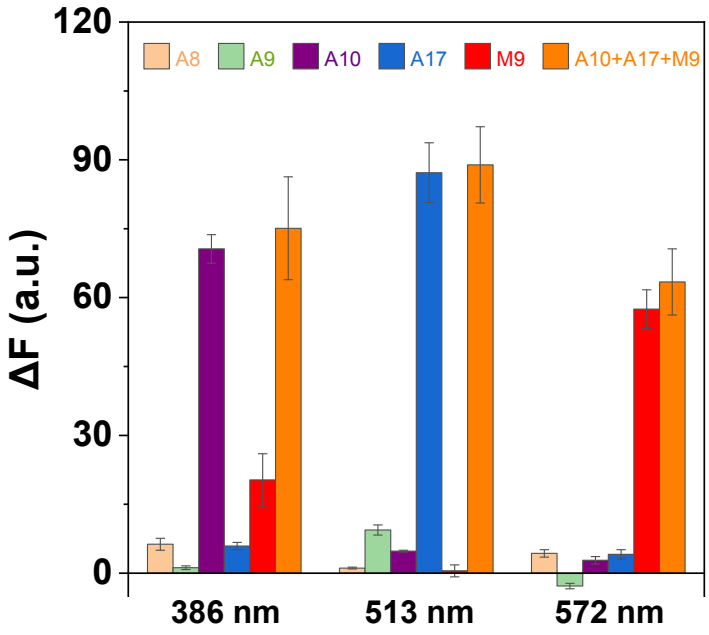

Figure 4. Selectivity of the nGO-COO-Peps sensor. The experiments were performed in the presence of individual standards of ADAM-8, ADAM-9, ADAM-10, ADAM-17, and MMP-9 as well as the mixture of ADAM-10, ADAM-17, and MMP-9 at $\lambda_{ex/em}$ = 321/386 nm, $\lambda_{ex/em}$ = 492/513 nm, and $\lambda_{ex/em}$ = 549/572 nm. The fluorescence intensity values were background corrected, which were obtained by subtracting the blank fluorescence intensity from that of the analyte species. The protease concentrations were 100 ng/mL each. Four separate experiments were performed for each sample.

TOC